

Testing and Modeling of Embedded Stainless Steel-Glass Connections

Rohola Rahnavard ^a, Eliana Inca-Cabrera ^a, Sandra Jordão ^a, Carlos Rebelo ^a

^a University of Coimbra, ISISE, ARISE, Department of Civil Engineering, Coimbra, Portugal,
rahnavard@uc.pt, e.inca.cabrera@uc.pt, sjordao@dec.uc.pt, crebelo@dec.uc.pt

Abstract

Embedded stainless steel–glass connections are widely used in transparent structures, but their mechanical behaviour depends on stress transfer through polymer interlayers. This study investigates an embedded stainless steel–glass detail with a polyvinyl butyral (PVB) interlayer and evaluates a finite-element model in Abaqus. Three laboratory tests were performed on identical specimens under monotonic loading. All specimens failed by delamination at the embedded interface. The model treats glass and steel as linear elastic, the PVB as a deformable interlayer, and uses an adhesive-zone (traction–separation) law to capture damage initiation and evolution. Geometric nonlinearity and contact simulate separation and post-peak behaviour. Predictions were compared with measurements, including global force–displacement response. The simulation reproduced stiffness, peak load, and post-peak softening across all three tests and correctly localised damage along the embedded edge. This close correspondence demonstrates the reliability of the modelling technique for assessing embedded steel–glass connections with PVB interlayers. The results provide a validated basis for parametric studies and predictions of capacity and failure modes in laminated glass assemblies.

Keywords

Cohesive zone formulation, Embedded connection, Finite element modelling, Laminated glass.

Article Information

- Digital Object Identifier (DOI): [10.47982/cgc.10.759](https://doi.org/10.47982/cgc.10.759)
- Published by [Challenging Glass](#), on behalf of the author(s), at [Stichting OpenAccess](#).
- Published as part of the peer-reviewed [Challenging Glass Conference Proceedings](#), Volume 10, June 2026, [10.47982/cgc.10](https://doi.org/10.47982/cgc.10)
- Editors: Christian Louter, Freek Bos & Jan Belis
- This work is licensed under a [Creative Commons Attribution 4.0 International](#) (CC BY 4.0) license.
- Copyright © 2026 with the author(s)

1. Introduction

The structural use of glass has evolved significantly over the last three decades, shifting from a purely infill material toward a primary load-bearing component in structures (Rahnavard and Jordao, 2026) and façades (Inca-Cabrera et al., 2025), roofs, floors, and bridges. Despite these advancements, the design of reliable and efficient connections remains one of the most critical challenges in structural glass engineering. Owing to the brittle nature of glass, stress concentrations at mechanical fasteners, particularly drilled holes for bolted joints, can significantly reduce structural capacity and trigger premature fracture. Consequently, alternative connection strategies that reduce local stress peaks and enable more distributed load transfer mechanisms have attracted growing attention in recent years (Haldimann et al. 2008; Louter et al. 2012; Bedon and Santarsiero 2018).

Among these alternatives, embedded laminated glass connections have emerged as a promising solution. In this approach, metallic inserts are incorporated directly within the laminated glass build-up during the lamination process, allowing forces to be transferred through the polymer interlayer rather than through discrete mechanical fasteners. This configuration enhances structural transparency, eliminates the need for drilling, and potentially improves stress distribution within the glass plies. Previous investigations have demonstrated the mechanical feasibility of such systems and highlighted the influence of insert geometry, glass thickness, and interlayer properties on connection stiffness and strength (Santarsiero et al. 2017; Santarsiero et al. 2018). Experimental pull-out tests and corresponding finite element analyses have shown that embedded connections can achieve substantial load-carrying capacity while maintaining favourable aesthetic integration (Santarsiero et al. 2018).

A key component governing the behaviour of embedded laminated connections is the polymeric interlayer. Laminated glass typically consists of two or more glass plies bonded by materials such as polyvinyl butyral (PVB), ionoplast, or thermoplastic polyurethane. These interlayers provide post-fracture integrity by retaining glass fragments, but they also play a fundamental mechanical role by transferring shear and tensile stresses between adjacent materials. The viscoelastic nature of PVB, in particular, leads to temperature- and rate-dependent stiffness, which directly affects the global load–displacement response of laminated assemblies (Bennison et al. 1999; Botz and Hof 2010; Santarsiero et al. 2018). In embedded connections, the interlayer also serves as the bonding medium between glass and metallic inserts, making its adhesion, shear modulus, and deformation capacity key parameters in determining connection performance.

Although prior studies have established the feasibility of embedded laminated connections, further experimental validation and numerical calibration remain necessary to better understand their mechanical response under tensile loading and to improve predictive modelling strategies. In particular, quantitative comparisons between experimentally obtained load–displacement behaviour and detailed finite element simulations are essential for validating constitutive assumptions and boundary conditions used in design-oriented models.

The present study addresses this need by experimentally investigating the tensile behaviour of stainless steel inserts embedded in laminated glass, with PVB as the interlayer. A series of tensile tests was conducted to characterise the load–displacement response of the embedded connection system. The experimental curves were subsequently reproduced through numerical simulations, and the predicted responses were compared directly with the measured results. By combining controlled experimental testing with finite element modelling, this work aims to evaluate the accuracy of current

modelling approaches and to contribute to the reliable structural design of embedded laminated glass connections.

2. Experimental program

2.1. Specimen geometry

The tensile specimens consisted of a laminated glass panel with an embedded stainless steel insert, as shown in Fig. 1. Each specimen had an overall height of 500 mm and a width of 300 mm. The laminate build-up comprised two fully tempered glass plies, each 5 mm thick, bonded using PVB interlayers. The stainless steel insert was a 3 mm thick plate positioned centrally within the laminate and embedded over an anchorage length of approximately 100 mm. According to the sectional configurations (Fig. 1), the connection region incorporated a 4.52 mm PVB layer in the central laminated zone, while a local layered region around the embedded insert included an additional 0.76 mm PVB layer, providing bonding and stress transfer between the steel and the adjacent glass plies. The stainless steel plate extended beyond the laminate to enable mechanical gripping, and the exposed steel regions contained bolt hole patterns ($\varnothing 26$ mm) used to connect the insert to the external steel loading fixtures. The embedment geometry was designed to promote load transfer primarily through interfacial shear stresses within the PVB layers rather than through direct bearing or mechanically fastened glass details.

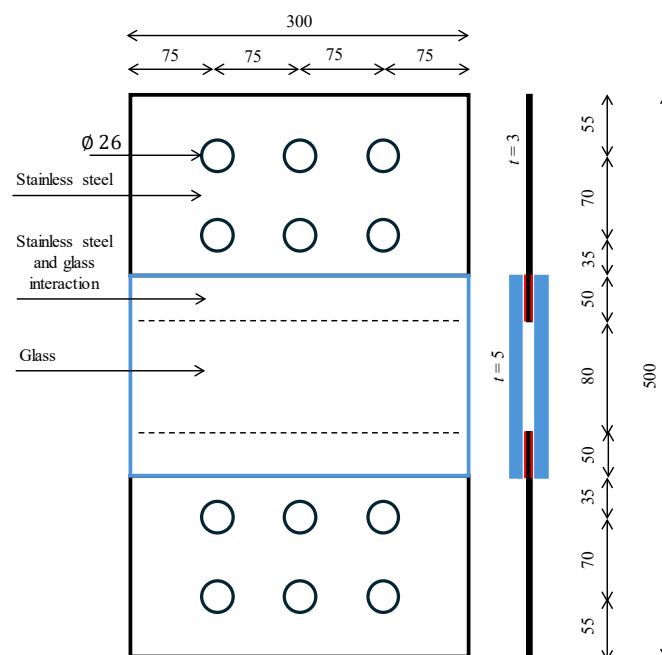


Fig. 1: Geometry of the embedded connections (units in mm).

2.2. Test setup

All tensile tests were conducted in a Shimadzu servo-hydraulic universal testing machine, using a vertical specimen arrangement as illustrated in Fig. 2. The laminated glass specimen was mounted through the protruding parts of the stainless steel insert, which were connected to the machine's upper loading head and lower base via custom rigid bolted steel fixtures. The gripping system comprised thick steel plates secured with high-strength bolts to ensure a stiff load path and stable clamping pressure, aiming to transfer the applied force concentrically to the embedded insert while

minimising eccentricity and secondary bending. Before each test, the alignment of the specimen and fixtures was checked to ensure that the tensile load was applied along the insert's longitudinal axis. The tests were performed under monotonic tensile loading in displacement control at a constant crosshead rate of 1 mm/min, which was selected to ensure quasi-static loading conditions and to minimize strain-rate effects associated with the viscoelastic behaviour of the PVB interlayer, and loading was continued until failure of the connection system. During the tests, the applied force was recorded by the machine's calibrated load cell, while global displacement was measured from the crosshead displacement; in addition, local response was monitored using digital image correlation and the installed electrical sensors (e.g., strain gauges) visible in the setup, which were connected to a data acquisition system. Visual observations were made throughout loading to identify the onset of damage and the governing failure mechanism, including possible interfacial debonding at the steel–PVB interface, progressive slip of the embedded insert, and/or fracture of one or both glass plies.

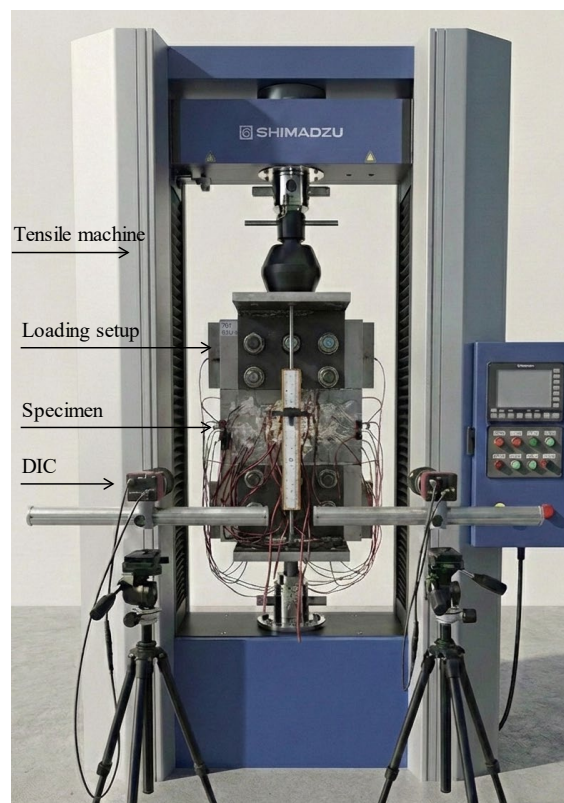


Fig. 2: Tensile test setup.

2.3. Experimental results

Fig. 3 presents the load–displacement curves obtained from the three tensile tests (Test 1–Test 3). The displacement in Fig. 3 was driven from the displacement measurement of the universal testing machine. The specimens exhibited consistent global behaviour, with similar stiffness evolution, peak load levels, and failure patterns. The response can be divided into three characteristic stages, corresponding to distinct mechanical mechanisms governing the behaviour of the embedded laminated connection.

At the initial stage of loading, the response was approximately linear up to a displacement of about 2.1 mm. This initial slope is attributed primarily to the prestressing effect of the bolted steel gripping system. Due to a clearance of approximately 1 mm on each side between the bolts and the holes, the

early deformation corresponded to the gradual closure of this gap and mobilisation of the clamping system rather than direct shear transfer through the embedded interface. Consequently, this portion of the curve does not fully represent the intrinsic stiffness of the embedded glass–PVB–steel connection, but rather the compliance of the mechanical loading assembly.

After closure of the bolt clearance, a change in slope was observed, marking the onset of direct load transfer through the embedded stainless steel insert and the surrounding PVB interlayer. In this stage, the behaviour was governed by shear stresses developing along the steel–PVB interface. The response remained stable and approximately linear until progressive interfacial degradation initiated within the PVB layer. With increasing displacement, localised slip of the steel insert began to occur, reflected in a gradual reduction in stiffness as the load approached its maximum value. This behaviour was visually confirmed during the tests by observing the relative movement of the steel insert with respect to the glass specimen near the embedded region.

The average maximum load recorded before the sudden load drop was 37.5 kN, with a standard deviation of 4.8 kN, indicating acceptable repeatability among the three specimens. At peak load, a sudden reduction in force exceeding 5% was observed in all tests. This abrupt drop corresponds to interfacial failure and rapid delamination of the PVB interlayer along the embedment length. Following this event, the load decreased sharply and stabilised at a lower residual level, attributed to frictional resistance between the steel insert and the partially detached interlayer.

Post-test inspection confirmed that all failures were governed exclusively by delamination at the steel–PVB interface (Fig. 4). No cracking was observed in the glass plies, and no plastic deformation was detected in the stainless steel insert or around the bolt holes. The steel plate and its perforations remained elastically deformed, indicating that the ultimate capacity of the system was controlled by the shear and adhesion capacity of the PVB interlayer rather than by the yielding of the metallic insert or the tensile fracture of the glass. Although the load–displacement response shows a sudden load drop, the observed behaviour differs from classical brittle glass failure since no cracking occurred in the glass plies. Instead, failure was governed by delamination of the PVB interlayer at the steel interface. Compared to glass fracture, this failure mode is less critical as it prevents catastrophic glass breakage and maintains specimen integrity. From a structural design perspective, a more ductile failure governed by steel yielding could be preferable; however, in the present configuration the connection capacity was controlled by the interfacial strength of the PVB layer rather than the strength of the stainless steel insert.

The observed failure mode and consistent load–displacement behaviour demonstrate that the structural performance of the embedded connection under tensile loading was governed by interfacial shear transfer within the PVB layer. The absence of glass cracking and steel yielding confirms that the laminate configuration and embedment geometry successfully shifted the critical mechanism toward interlayer delamination, thereby preventing brittle glass failure.

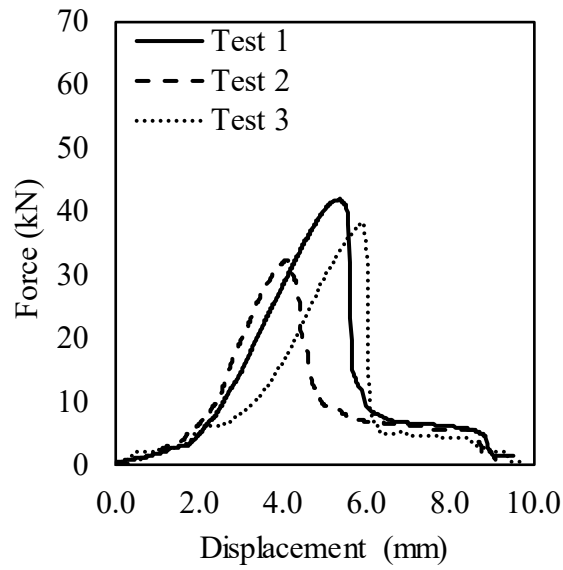


Fig. 3: Experimental load vs displacement curves.

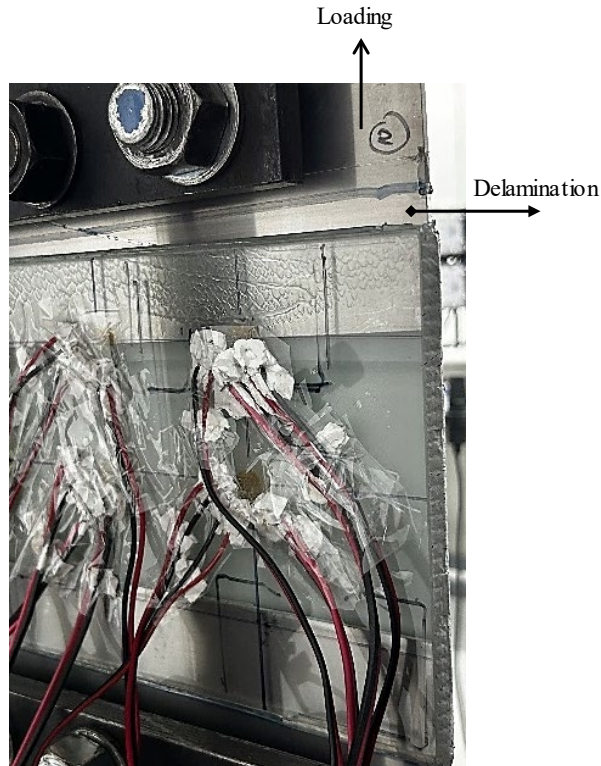


Fig. 4: Failure mode of test 1.

3. Numerical simulations

A three-dimensional finite element model of the experimental configuration was developed in Abaqus to reproduce the tensile tests and better understand the load-transfer mechanisms governing the embedded laminated glass connection. The numerical model included both the specimen and the loading fixtures to accurately represent the boundary conditions and the stiffness contribution of the test assembly. To reduce computational effort while maintaining accuracy, geometric symmetry was

exploited, and symmetry boundary conditions were applied in the X, Y, and Z directions, allowing only the representative portion of the setup to be analysed while preserving the global structural response. All components, including the glass plies, PVB interlayers, stainless steel insert, clamping plates, and bolts, were discretised using three-dimensional 8-node reduced integration solid elements (C3D8R). A refined mesh was adopted in the embedded region to capture stress concentrations and progressive interfacial damage. The PVB interlayer was modeled using C3D8R solid elements with a simplified linear elastic material model assuming a Poisson's ratio of 0.47. Since the material was not treated as fully incompressible and large strain effects were not considered, hybrid elements were not adopted.

The analysis was performed in two sequential steps reflecting the experimental procedure. In the first step, bolt preload was introduced to simulate the tightening of the clamping system and to reproduce the initial stiffness associated with the closure of bolt-hole clearances observed in the tests. In the second step, a monotonic tensile displacement was applied to the loading head under displacement control until the connection failed. Contact interactions between steel components, including plates and bolts, were defined using hard normal contact and a tangential Coulomb friction coefficient of 0.3. The interaction between the glass, PVB interlayer, and stainless steel insert was modelled using a cohesive zone formulation that incorporates damage initiation and progressive degradation to simulate interfacial delamination.

Fig. 5 illustrates the finite element model and the interaction definitions, while Fig. 6 compares the numerical and experimental load–displacement responses. The simulation reproduced the global behaviour of the connection, including the initial stiffness, peak load, and post-peak softening associated with interfacial failure. A close agreement between experimental measurements and numerical predictions was achieved, indicating that the adopted modelling strategy and cohesive interface representation successfully captured the governing failure mechanism of the embedded laminated glass connection.

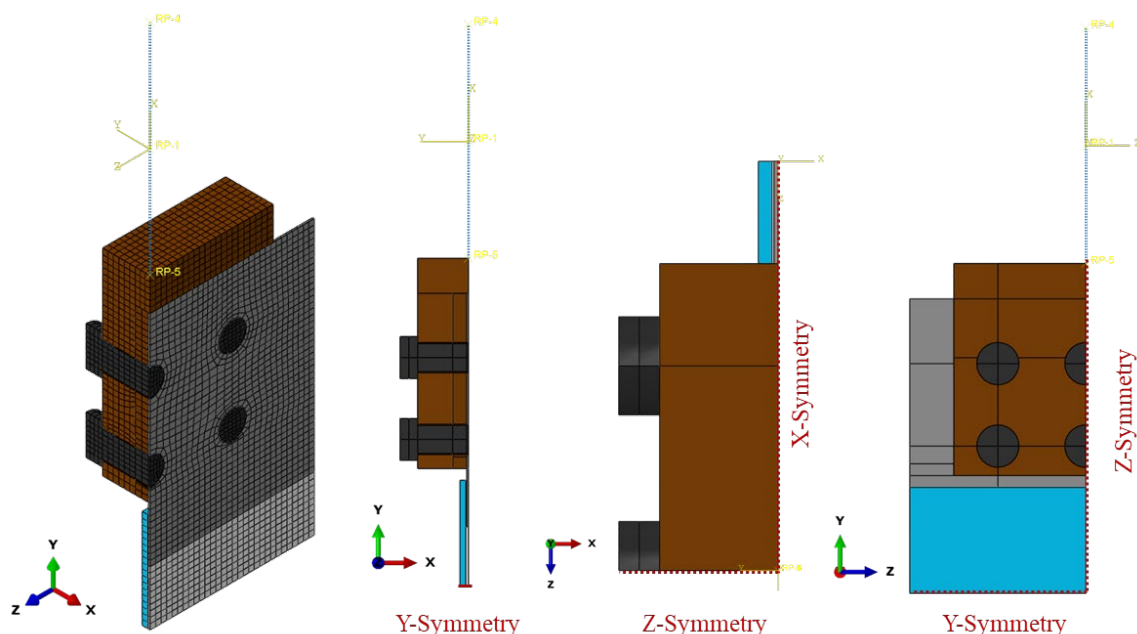


Fig. 5: Simulation of the embedded connection with the symmetry technique.

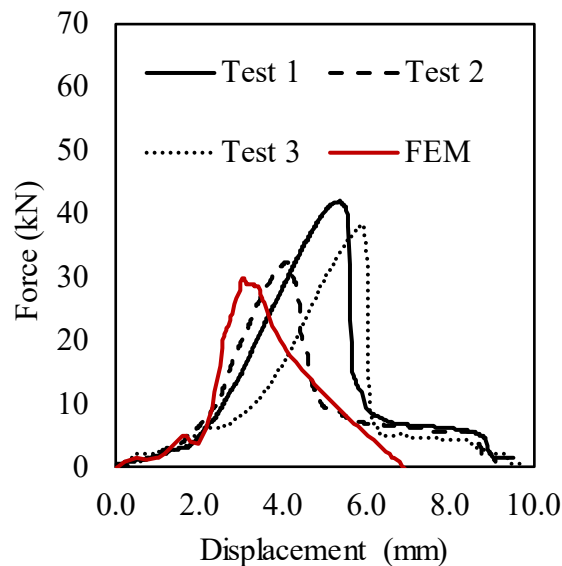


Fig. 6: Comparison of experimental and numerical results.

4. Conclusion

An experimental and numerical investigation was conducted to examine the tensile behaviour of a stainless steel insert embedded in laminated glass with a PVB interlayer as the bonding medium. Three monotonic tensile tests were performed, and the load–displacement responses were compared with finite element simulations developed in Abaqus.

The experimental results showed a consistent mechanical response for all specimens. An initial linear stiffness was observed up to approximately 2.1 mm of displacement, attributed to the closure of the bolt–hole clearance and the mobilisation of the clamping system. After this stage, the load was transferred directly through the embedded connection and governed by shear stresses within the PVB interlayer. The specimens reached an average maximum load of 37.5 kN with a standard deviation of 4.8 kN. Failure occurred through delamination at the steel–PVB interface, followed by a sudden drop in load capacity. No cracking was observed in the glass plies, and no plastic deformation occurred in the stainless steel insert or in the bolt holes, confirming that the ultimate resistance of the system was controlled by interfacial adhesion within the interlayer rather than by glass fracture or steel yielding.

A three-dimensional finite element model including the specimen and the loading assembly was developed using solid elements and cohesive interface behaviour to simulate interfacial damage and separation. The analysis incorporated bolt preload and subsequent tensile displacement to replicate the experimental procedure. The numerical model successfully reproduced the stiffness evolution, peak load, and post-peak behaviour of the connection. The comparison between experimental and numerical load–displacement curves showed close agreement, demonstrating that the cohesive zone modelling approach is suitable for capturing the governing delamination mechanism.

Overall, the study confirms that embedded laminated glass connections can transfer tensile forces without inducing brittle glass fracture, with the structural performance governed by the shear capacity of the PVB interface. The validated numerical model provides a reliable tool for predicting the behaviour of similar embedded connections and may support future design and optimisation of load-bearing glass assemblies.

Acknowledgements

The authors gratefully acknowledge the support of the “R2UTechnologies | modular systems” innovation project (operation code 01/C05-i11/2024.PC644876810-0000019), funded under the Portuguese Recovery and Resilience Plan (PRR) through the NextGenerationEU programme. This work was partly financed by FCT / MCTES through national funds (PIDDAC) under the R&D Unit Institute for Sustainability and Innovation in Structural Engineering (ISISE), under reference UID/04029/Institute for Sustainability and Innovation in Structural Engineering (ISISE), and under the Associate Laboratory Advanced Production and Intelligent Systems ARISE under reference LA/P/0112/2020.

References

- Rahnavard, R., Jordão, S., *Testing and simulation of simple and prestressed laminated glass beams*, Composite Structures, Volume 378, 2026, 119924, <https://doi.org/10.1016/j.compstruct.2025.119924>.
- Inca-Cabrera, E., Jordão, S., Rebelo, C., Bedon, C., Mesquita, A., Hosseini, S.A., *Experimental and numerical investigation of in-plane cyclic response of a point-fixed glass façade system for seismic performance assessment*, Journal of Building Engineering, Volume 108, 2025, 112956, <https://doi.org/10.1016/j.jobbe.2025.112956>.
- Haldimann, M., Luible, A., Overend, M.: *Structural Use of Glass*. IABSE, Zurich (2008). doi:10.2749/sed010
- Louter, C., Belis, J., Veer, F.: Structural glass connections: a review of experimental research and design methods. *Heron* 57(3), 203–228 (2012)
- Bedon, C., Santarsiero, M.: Transparency in Structural Glass Systems via Mechanical, Adhesive, and Laminated Connections – Existing Research and Developments. *Advanced Engineering Materials* 20(5), 1700815 (2018). doi:10.1002/adem.201700815
- Santarsiero, M., Louter, C., Nussbaumer, A.: Laminated connections for structural glass components: a full-scale experimental study. *Glass Structures & Engineering* 2, 45–69 (2017). doi:10.1007/s40940-016-0033-2
- Santarsiero, M., Bedon, C., Louter, C.: Experimental and numerical analysis of thick embedded laminated glass connections. *Composite Structures* 188, 242–256 (2018). doi:10.1016/j.compstruct.2018.01.002
- Bennison, S.J., Jagota, A., Smith, C.A.: Fracture of glass/poly(vinyl butyral) laminates in biaxial flexure. *Journal of the American Ceramic Society* 82(7), 1761–1770 (1999). doi:10.1111/j.1151-2916.1999.tb01997.x
- Botz, M., Hof, P.: Mechanical behaviour of PVB interlayers under different loading and temperature conditions. *Glass Processing Days Conference Proceedings*, Tampere, 323–326 (2010)

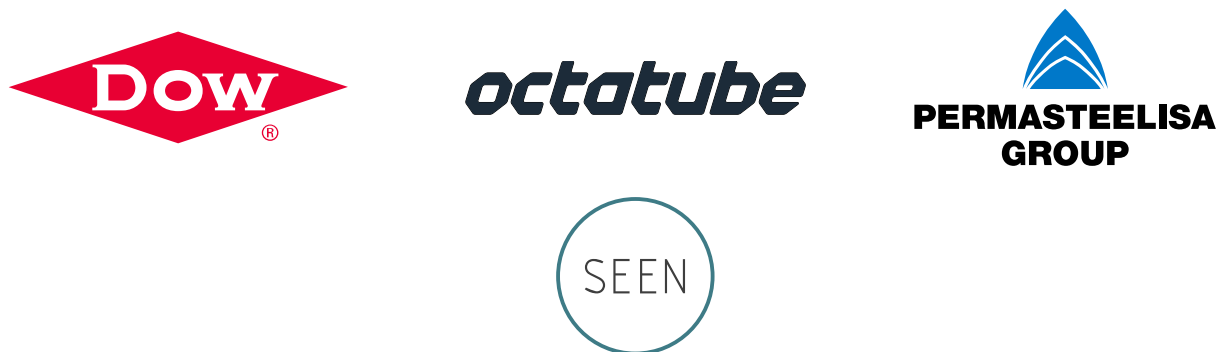
Platinum Sponsor



Gold Sponsors



Silver Sponsors



Organisation

